DOI: 10.1002/cphc.201000917

Monitoring the Backbone Conformation of Valinomycin by Raman Optical Activity

Shigeki Yamamoto,*[a] Hitoshi Watarai,[b] and Petr Bouř*[a]

Raman optical activity (ROA) spectroscopy is used to investigate the backbone conformation of valinomycin in methanol and dioxane solution. Experimental Raman and ROA spectral differences are interpreted by using density functional calculations, molecular dynamics, and Cartesian tensor transfer. Of the several conformers with different numbers of intramolecular hydrogen bonds which were preselected by calculations of relative energies, the dominant ones are identified on the basis of ROA. To separate the backbone signal from that of the side chains, conformational search for the isopropyl residues is performed for each backbone conformer. In dioxane, the most populated conformer does not exhibit C_3 symmetry, but adopts a distorted "bracelet" structure, similar to a crystal structure. This complements previous NMR spectroscopic results that could not distinguish the nonsymmetric structures. In methanol, a different, "propeller" conformer is indicated by ROA, which has three loops resembling a standard β-turn peptide motif. Molecular dynamics simulations suggest that the propeller structure is very flexible in methanol. Spectra simulated for geometries not having the β-turn do not agree with experiment. On the basis of these results, a distinct +/− ROA couplet at ~1335/1317 cm^{-1} observed in the extended amide III region is assigned to a turn in the valinomycin backbone.

1. Introduction

Valinomycin is a hydrophobic antibiotic that can carry potassium ions through biological membranes.[1,2] The molecule is cyclic, and contains twelve acids with a threefold repeating motif, (L-Lac-L-Val-D-Hiv-D-Val)$_3$, where Val, Hiv, and Lac are valine, α-hydroxyisovaleric acid, and lactic acid, respectively. The backbone geometry is very similar to a peptide chain because of the similarity of the amide and ester linkages. Transport of ions is dependent on complex formation between free valinomycin and the cation on the membrane surface.[3] Complexation induces a conformational transition, resulting in a hydrophobic complex that can penetrate the membrane. The conformational transition depends on the polarity of the environment. To better understand the conformational forms, and also to explore the potential of Raman optical activity (ROA) spectroscopy, we monitored valinomycin conformations in two solvents (dioxane and methanol) by a combination of spectroscopy and multiscale molecular modeling.

ROA is a polarized Raman technique. It measures a tiny difference in scattering of right and left circularly polarized light.[4–7] This method can provide not only absolute configuration, such as that of the Van't Hoff asymmetric carbon atoms, but also information about the particular conformation of a chiral molecule in solution.[8–12] The vibrational transitions monitored by ROA are usually more numerous, and thus provide more information than the electronic ones.[6,7] Recent improvements in ROA instruments[13,14] and advanced interpretation methods[15] allow one to obtain detailed structural information, at least for small molecules. For larger proteins, however, experimental spectra must often be interpreted empirically. For example, spectra of proteins of known structure are used to determine Raman and ROA marker bands characteristic of a particular structural feature.[7,10,16–18] Of course, for more reliable structure determinations theoretical simulations of the spectra for larger molecules are desirable, too. Valinomycin is a convenient intermediate-sized model for which the usefulness of ROA for backbone structural monitoring can be documented. Its solution forms are very flexible, and there is a limited number of methods that provide information about the conformational equilibria in the liquid sample.

In a previous study,[19] we investigated the extreme sensitivity of ROA spectroscopy to the isopropyl side-chain conformation in the potassium–valinomycin complex, confirmed by comparison of the experimental and calculated data. Characteristic ROA peaks of the complex, in particular a sharp +/− ROA couplet around 1325 cm^{-1}, that is, in the extended amide III region of 1400–1300 cm^{-1},[10,20] was successfully reconstructed by the computations. However, the backbone conformational change following complexation could be monitored only roughly. In particular, the experimental ROA spectrum of free valinomycin in methanol was not reproduced well. Monitoring of the backbone conformation of free valino-

[a] Dr. S. Yamamoto, Dr. P. Bouř
Institute of Organic Chemistry and Biochemistry
Academy of Sciences, 166 10 Prague (Czech Republic)
Fax: (+420) 220183578
E-mail: aporoa@gmail.com
bour@uochb.cas.cz

[b] Prof. H. Watarai
Department of Chemistry, Graduate School of Science
Osaka University, Toyonaka
Osaka 560-0043 (Japan)

Supporting information for this article is available on the WWW under http://dx.doi.org/10.1002/cphc.201000917.

mycin by ROA is more difficult because the pseudo-peptide chain is more flexible than in the complex, and the backbone spectral signal overlaps with that of the side chains. Nevertheless, as shown below, comparison of the spectra obtained with different solvents and coupling of quantum modeling and molecular dynamics make prediction of the backbone conformation more reliable.

Previous works[2,19,21,22] suggest that complexed valinomycin in solution has almost the same backbone structure as in the crystal.[23] The complex adopts a symmetric bracelet-like form in which all six ester carbonyl groups are strongly bound to the potassium ion in a central cavity. The structure is further stabilized by six intramolecular 4→1 hydrogen bonds between NH and amide C=O. It is thus isomorphous with peptide β-turns (Figure 1), at least with respect to the main-chain torsion angles. Three of the turns are composed of the L-Lac-L-Val-D-Hiv-D-Val sequence, whereas the other three are formed by D-Hiv-D-Val-L-Lac-L-Val.[24]

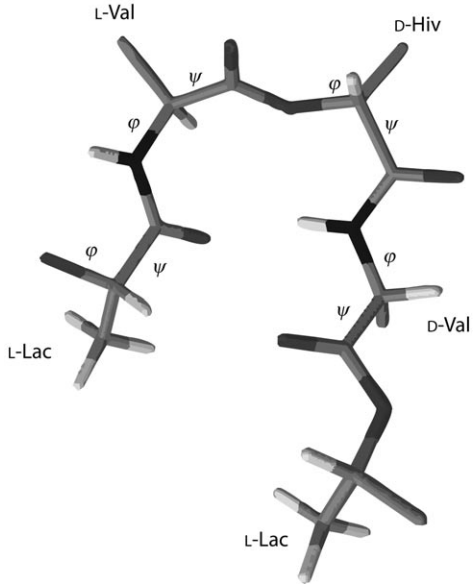

Figure 1. Typical type II β-turn structure found in the optimized structures of the bracelet and the propeller conformers of valinomycin. Isopropyl side groups were removed for clarity, the main backbone torsion angles (φ, ψ) are indicated.

Free valinomycin can be crystallized with formation of several conformers, such as asymmetric bracelet form (from *n*-octane)[25] and a propeller form (from dimethyl sulfoxide, DMSO).[26] The structure of the asymmetric bracelet is close to that of the potassium complex. Five 4→1 hydrogen bonds stabilize this structure, and one NH group binds to the ester C=O group (5→1 hydrogen bond). In the propeller structure, only three intramolecular 4→1 hydrogen bonds remain between the NH group of D-Val and C=O of L-Lac. Three β-turns are present in the L-Lac-L-Val-D-Hiv-D-Val sequences.

In solution, free valinomycin adopts variable conformations depending on solvent polarity.[2,21,22,27] A symmetric bracelet form was proposed as the dominant structure in nonpolar solvents such as cyclohexane and chloroform.[21] A propeller structure was suggested for solvents of medium polarity, such as CCl_4/DMSO (3/1)[21] or dioxane.[22] The NMR coupling constants and molecular modeling were used as evidence. However, it is known that in both nonpolar and polar solvents dynamic conformational equilibria of valinomycin occur with relaxation times shorter than 10^{-6} s.[27] In such a case, NMR spectroscopy cannot distinguish the conformers due to its relatively slow response time. On the other hand, due to the fast response of ROA (Raman scattering process), the optical spectrum is an algebraic sum of individual conformer subspectra.

The most universal way to interpret ROA spectra is by quantum mechanical calculations.[6,7,15] Development of calculation methods in the last decades[15,28–32] made it possible to achieve excellent agreement between experiment and theory, at least for small and rigid molecules.[33–35] Recently, ROA simulation of a protein segment containing over 400 atoms was reported.[36] Still, calculations on large molecules require significant effort, especially for flexible systems, for which many conformers must be considered. In such cases, the Cartesian coordinate tensor transfer (CCT) technique[37] can be applied to obtain results with nearly full ab initio accuracy, but in a shorter time.[38] In CCT, the force field (determining vibrational frequency) and intensity tensors are usually calculated at a high level of approximation for small fragments, and transferred to the target molecule. This methodology has been successfully applied to simulations of both vibrational circular dichroism (VCD)[39,40] and ROA[12,19] spectra, including ROA of flexible molecules.[41–43] A database of characteristic fragments can be used for many conformers with a similar structure.[41]

The B3LYP[44] functional was previously used to calculate accurate force field and polarizability tensors of valinomycin.[19] In this study, we used the similar B3PW91[45] functional, which better reproduces some minor spectral features, such as the methyl deformation ROA band at about 1460 cm^{-1} and low-frequency region of extended amide III ROA bands at about 1390 cm^{-1}. This is important for monitoring the backbone structure, as these bands appear to be extremely sensitive to backbone variations. A detailed comparison of the performances of the B3PW91 and B3LYP functionals for vibrational properties can be found elsewhere.[46–48]

Experimental and Computational Section

Experimental Methods: Valinomycin was purchased from Sigma and recrystallized twice from methanol. Similarly to potassium,[19] another complex of valinomycin giving almost the same spectrum was prepared by dissolving molar equivalents of RbCl (Aldrich) and valinomycin in methanol. The solution of free valinomycin in methanol contained equivalents of LiCl (Fluka, note that lithium does not form any complex with valinomycin). The initial concentrations of valinomycin were 0.10 M in methanol and 0.37 M in dioxane. For the dioxane solution, precipitation occurred after a pre-irradiation by the laser, but the remaining solution could be used for the ROA measurement. Based on the resultant Raman intensity of valinomycin per unit laser power and the acquisition time, we estimate the final concentration of valinomycin in dioxane to be close to 0.1 M, that is, similar to that in methanol. The ROA spectra were mea-

sured with a backscattered circularly polarized instrument at the University of Fribourg[13,14] with 532 nm excitation wavelength, and 7 cm^{-1} spectral resolution. The laser powers at the sample were 400 mW for methanol and 200 mW for dioxane solutions. To exclude artifact signals in ROA intensities, the measurements were repeated three times for slightly different positions of laser focus. Total acquisition times for the complex and the free compound in methanol and dioxane were 10, 3, and 6 h, respectively. Other experimental details were the same as in reference [19]. Solvent peaks and fluorescence background were subtracted from the Raman spectra; raw Raman spectra can be found in Figure S12 of the Supporting Information. Third-order nine-point Savitzky–Golay smoothing was applied to the ROA spectra. The ROA and Raman intensities are presented in units of electrons detected by the CCD camera.

Molecular Dynamics: The Tinker program package[49] with the Amber99 force field[50] was used to estimate the backbone flexibility and its influence on the ROA and Raman spectra. A similar procedure as in reference [19] was used for annealing and propagation of valinomycin, with a cubic periodic solvent box with 3 nm a side. The X-ray geometry of free valinomycin[26] was used as starting structure. For the propeller conformer, the lengths of the hydrogen bonds between NH of D-Val and C=O of L-Lac were fixed to those in the crystal (0.2165 nm). For other structures no restrictions were applied.

Conformation Search on Isopropyl Side Chains: As shown before[19] the ROA spectrum of valinomycin strongly depends not only on the backbone, but also on the side-chain isopropyl torsion angles. The torsion angle was defined as $\angle H_\alpha C_\alpha C_\beta H_\beta$, as in the previous study.[19] We searched for the stable isopropyl torsion angles for each backbone conformation, through 120° angular increments. In the case of the complex, the conformational search could be done at lower computational levels (e.g., AM1 or PM3).[19] The strong interaction between potassium ion and valinomycin made the backbone structure stable. However, these levels appeared too inaccurate for free valinomycin; in particular, they unrealistically destroyed the planarity of the peptide groups. Thus the BPW91/6-31G** approximation was chosen to take consistently into account both the intramolecular hydrogen bonds and the side-chain interactions.

Considering only three possible torsion angles (ca. −60, 60, 180°) of the nine isopropyl groups of valinomycin, $3^9 = 19683$ conformers are possible for each backbone conformation. Even for a C_3-symmetrical backbone structure, 6579 unique structures can be generated by isopropyl rotation. Because it is currently unrealistic to reliably optimize all these conformers (i.e. at the BPW91/6-31G** level), we presumed that the isopropyl groups of D-Hiv adopt an angle of about 60°. The value of 180° is sterically not allowed, because the isopropyl group of D-Hiv would be sandwiched between two isopropyl groups of L-Val and D-Val; additionally, in the complex,[19] no stable conformer with an angle of 180° for D-Hiv was found. The third possible angle of about −60° systematically provided higher energies due to a different steric hindrance, caused by the amide carbonyl group of D-Hiv filling the space between D-Hiv and D-Val (Figure S1, Supporting Information). The preference for 60° was also indicated by the potential-energy scan of the isopropyl angle of D-Hiv in the L-Val-D-Hiv-D-Val fragment, performed at the BPW91[51]/6-31G** level with the Gaussian program suite[52] (Figure S2, Supporting Information).

Theoretical ROA and Raman Spectra: The spectra were calculated with the Gaussian program suite.[52] Smaller fragments were created from selected valinomycin conformers, and partially optimized in the normal-mode coordinates.[53,54] Vibrational modes of harmonic frequencies between *i*300 (imaginary) and 300 cm^{-1} were kept constant to avoid large deviations from the original structure determined by MD. The force field and derivatives of the electric dipole–electric dipole polarizability ($\boldsymbol{\alpha}$, giving the Raman intensities) were calculated at the B3PW91/PCM(MeOH)/6-31++G** level for the fragments and transferred to the whole valinomycin molecule by the CCT method.[37] Local derivatives (placed in origins at the nuclei) of the ROA intensity tensors ($\mathbf{G}'$ and $\mathbf{A}$) were calculated for the whole molecule at the HF/6-31G level, whereas the origin-dependent parts were taken from $\boldsymbol{\alpha}$. Full construction of $\mathbf{G}'$ and $\mathbf{A}$ from fragments was thus avoided because of the larger error introduced by the fragmentation in this case.[19] Backscattering Raman and ROA spectra were generated from the intensities by using Lorentzian peaks with line widths of 5 cm^{-1} and including the Boltzmann temperature correction for 300 K. The experimental ROA spectra were decomposed into the calculated spectra by using the least square fitting described elsewhere.[11,55]

2. Results and Discussion

2.1. Experimental Spectra

The experimental ROA and Raman spectra of free valinomycin in methanol and dioxane and of the Rb complex of valinomycin in methanol are plotted in Figure 2. Because the spectra of the rubidium complex are quite close to those of the potassium complex described before,[19] we can suppose that the valinomycin conformations are also similar. However, we note that the presence of LiCl or NaCl in the methanol solutions, for example, did not affect the spectra of free valinomycin, in accord with the known low affinity of valinomycin to these ions.[2]

The most distinct spectral changes caused by complexation occur in the extended amide III region (1400–1200 cm^{-1}). The complexed form has a sharp +/− ROA couplet at 1335/1317 cm^{-1}, whereas free valinomycin exhibits a broader +/−/+ "W-shaped" structure at 1345/1305/1265 cm^{-1}, both in methanol and dioxane. In dioxane, two distinct positive ROA peaks exist at 1353 and 1335 cm^{-1}. Previous analyses of similar flexible molecules[11,41,56,57] suggest that the broadened ROA peaks of the free form probably accompany many conformational species of valinomycin in solution.

The free-molecule spectra in dioxane and methanol are also different. Unlike methanol, dioxane is a relatively nonpolar solvent. It can accept hydrogen bonds but does not have acidic hydrogen atoms. Interestingly, however, some ROA spectral features of free valinomycin in dioxane are similar to those of the complex in methanol. Both systems exhibit a −/+/− pattern of the methyl deformation bands at about 1470/1459/1447 cm^{-1}, a negative peak of the isopropyl group at about 1000 cm^{-1}, and a positive amide V peak at about 345 cm^{-1}. There are also similarities in the Raman spectra, for example, at the amide I bands, and a band at about 485 cm^{-1}. In methanol, characteristic ROA peaks are absent for free valinomycin, such as the highest-frequency negative peak of the methyl deformation band at 1470 cm^{-1}, the isopropyl peak at about 1000 cm^{-1}, and the amide V ($\delta(NH)_{op}$) peak at about 345 cm^{-1}. Thus a naive empirical comparison of the experimental spectra may mean that the structures of the free form in dioxane and

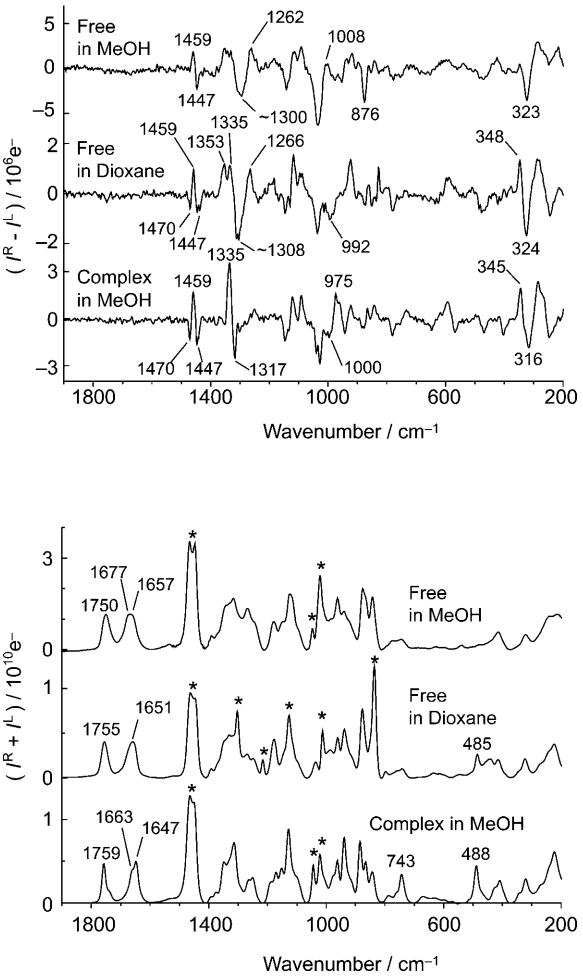

Figure 2. Experimental ROA (top) and Raman (bottom) spectra of free valinomycin in methanol and dioxane and of valinomycin complex in methanol. Solvent peaks and the fluorescence background were subtracted from the Raman spectra. Asterisks in Raman spectra indicate peaks that strongly overlap with those of the solvents. The intensity is presented as number of electrons detected by CCD.

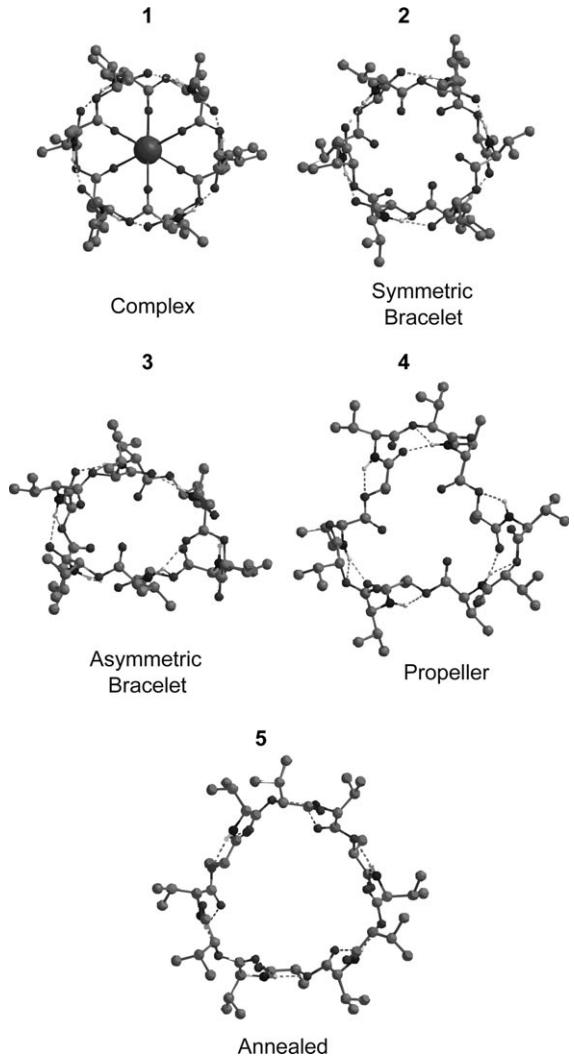

Figure 3. The discussed valinomycin forms. The complex, asymmetric bracelet, and propeller geometries are based the crystal structures with PDB codes of VALINK,[23] VALINO,[25] and GEYHOH.[26] The symmetric bracelet structure was obtained by optimizing the complex form without the metal ion. The annealed structure was found in the MD simulation without any restriction on the force field. All structures were optimized at the BPW91/6-31G** level. For clarity hydrogen atoms were removed from the side chains.

the complex are similar, at least in the neighborhood of the methyl and NH groups.

In all ROA spectra the amide I band (C=O stretching, ca. 1677 cm^{-1}) is very weak, hidden in the noise. The ROA peaks of the amide I band are usually observed in the spectra of proteins[10] and also in small flexible peptides.[43,58,59] We explain the absence of this band by the internal achirality (planarity) of the amide and ester chromophores, weak interaction among the carbonyl groups, and by the molecular flexibility.

2.2. Backbone Structures of Free Valinomycin

The NMR and X-ray data and MD simulations described above provided the preferred classes of conformers displayed in Figure 3. Their geometries were optimized by energy minimization at the BPW91/6-31G** level; the backbone angles of the minima defined in Figure 1 are listed in Table 1.

The complexed form of valinomycin, based on the crystal structure,[23] maintained its six-β-turn-like structure also during optimization. These turns can be associated with two peptide canonical types: three of the L-Lac-L-Val($\varphi_{i+1}=-64^\circ$, $\psi_{i+1}=133^\circ$)-D-Hiv($\varphi_{i+2}=81^\circ$, $\psi_{i+2}=11^\circ$)-D-Val sequences form the type II β-turn, whereas three D-Hiv-D-Val($\varphi_{i+1}=63^\circ$, $\psi_{i+1}=-134^\circ$)-L-Lac($\varphi_{i+2}=-80^\circ$, $\psi_{i+2}=-11^\circ$)-L-Val units adopt the type II′ turn.[24]

The symmetric bracelet structure was obtained by optimizing the complex without the central potassium ion. This backbone structure is stabilized by six intramolecular 4→1 hydrogen bonds between NH and amide C=O, and thus maintains the repeating six β-turn structures.

The asymmetric bracelet form was obtained from the crystal grown from *n*-octane;[25] the geometry was only slightly distorted in the free optimization. The optimized structure contains three type II and two type II′ β-turns.

Table 1. Calculated (BPW91/6-31G**) backbone torsion angles of valinomycin conformers.

	L-Val		D-Hiv		D-Val		L-Lac	
ID	φ	ψ	φ	ψ	φ	ψ	φ	ψ
				Complex				
calcd	−64	133	81	11	63	−134	−80	−11
				Symmetric bracelet				
calcd	−83	108	120	−3	81	−109	−123	7
NMR[a]	−80	90	120	0	60	90	180	−120
NMR[b]	30	60	100	−60	−40	−60	−100	60
				Asymmetric bracelet				
calcd	−74	21	103	3	89	−90	−137	2
	−90	94	132	3	68	−128	−112	15
	−63	130	77	6	107	−79	−155	37
X-ray[c]	−107	81	143	−11	59	−128	−93	2
	−63	130	74	9	109	−73	−160	27
	−66	125	96	2	63	−129	−70	−15
				Propeller				
calcd	−80	107	114	−5	118	−166	−141	17
X-ray[d]	−86	112	100	5	122	−173	−140	53
	−83	117	85	9	126	179	−137	23
	−64	121	91	−4	133	177	−143	41
NMR[a]	−85	100	120	0	110	90	−120	120
NMR[b]	30	90	100	−60	140	100	−100	90
				Annealed				
calcd	−131	165	119	5	131	−167	−145	4
NMR[b,e]	−140	70	80	−60	140	−70	−90	60
	−150	140	90	−80	150	−140	−100	80

[a] Ref. [21]. [b] Ref. [22]. [c] PDB code: VALINO.[25] [d] PDB code: GEYHOH.[26] [e] Range of angles indicated.

Table 2. Calculated relative energies of the lowest-energy backbone conformers of free valinomycin.

	E [kcal mol^{-1}]		
Conformer	BPW91/6-31G**	ZPE[a]	CPCM[b]
sB	0	0	0
asB	4.6	4.8	–[c]
P	16.5	15.8	10.3
A	17.7	16.5	8.8

[a] Zero-point energy correction, BPW91/6-31G**. [b] BPW91/6-31G**/CPCM(MeOH). [c] Optimized to the sB structure.

The propeller backbone structure of the crystal obtained from DMSO[26] did not change significantly during optimization. It has three intramolecular 4→1 hydrogen bonds, between the NH group of D-Val and C=O of L-Lac. Additional 2→1 hydrogen bonds, between NH of D-Val and ester oxygen atom (–O–) of D-Hiv, and NH of L-Val and ester O of L-Lac, also stabilize this conformation. The three turns present in the fragment, L-Lac-L-Val($\varphi_{i+1}=-80^\circ$, $\psi_{i+1}=107^\circ$)-D-Hiv($\varphi_{i+2}=114^\circ$, $\psi_{i+2}=-5^\circ$)-D-Val, are type II β-turns.[24]

The annealed structure was produced by MD annealing without any restriction on the force field (Figure S3, Supporting Information). The backbone angles were relatively stable during the 1 ns MD propagation, as documented by the time dependence in Figure S4 of the Supporting Information. The 4→1 intramolecular hydrogen bonds and β-turns were absent in this form, as stabilizing interactions between the methanol solvent and the backbone carbonyl groups prevailed. Only the 2→1 hydrogen bonds remained. The annealed MD geometry exhibited only minor changes when optimized in vacuo by the BPW91/6-31G** method. This conformation was proposed to be the dominant conformer in methanol, on the basis of combining measurements of NMR coupling constants and molecular modeling.[22]

The relative energies calculated for the four backbone structures are listed in Table 2. The most stable conformer appears to be the symmetric bracelet, both in vacuo and methanol, modeled by CPCM. It is more stable than the propeller and annealed conformers, by about 17 kcal mol^{-1}. The zero-point vibrational energy correction did not change the relative energies in vacuo significantly. This energy difference between the conformers is very large, but it could be well compensated by the hydrogen bonds between the valinomycin and solvent molecules, which were only partially taken into account by the continuum CPCM dielectric model. Formation of hydrogen bonds was observed during the MD run with the annealed structure, whereby about ten methanol molecules were always simultaneously involved in hydrogen bonding to the backbone carbonyl groups. Thus, while the available theoretical methods provide a good indication of valinomycin conformations, accurate discrimination between the conformers based on energetic arguments is impossible with current computational means. In particular, more precise MD calculations including explicit solvents molecules are desirable in future.[60–63] Fortunately, more insight can be obtained from the spectra (see below).

We abbreviated these most probable backbone conformations as sB for symmetric bracelet, asB for asymmetric bracelet, P for propeller, and A for the annealed conformer.

2.3. Conformations of the Isopropyl Residue

Detailed isopropyl torsional angles, found by a conformational search at the BPW91/6-31G** level, are listed in Tables S1–S4 of the Supporting Information, in which similar sets of torsional angles of the fragment L-Val-D-Hiv-D-Val are highlighted by the same color. The most stable side-chain conformations vary with the backbone structures. The "blue" set (ca. 180/60/180° for L-Val/D-Hiv/D-Val) is dominant for the bracelet, the "green" set (180/60/60°) for the propeller, and the "red" set (−60/60/60°) for the annealed geometry.

The populations (Tables S1–S4, Supporting Information) of the isopropyl conformers were calculated from the relative energies at 300 K. The energy differences are more subtle than those found for the different backbone conformers (Table 2). This corresponds to the weaker, mostly dispersionlike, forces by which the isopropyl groups interact with the solvent and other molecular parts. As these forces are relatively independent of solvent polarity, we suppose that the calculated isopropyl conformer energies can be used to predict reliable conformer distributions in our samples, as verified previously for the potassium complex of valinomycin.[19]

For the symmetric bracelet, two isopropyl conformers (sB1,2) dominate (with calculated populations of 69 and 27%; see

Table S1, Supporting Information), and the side chains behave similarly as in the complexed valinomycin.[19] This is reasonable, as the backbones are similar. For the asymmetric bracelet (without C_3 backbone symmetry) a systematic conformational search was not possible due to the vast number of possible conformers. However, given that the isopropyl torsional angles of asB2 are similar to those in the crystal, and that the torsion angles and energy ordering of asB1 and asB2 are nearly the same as for sB and the complex, we expect that asB1 and asB2 are the most stable forms.

The lowest-energy isopropyl conformers of the propeller and annealed structures are listed in Tables S3 and S4 of the Supporting Information. Because of the larger distances between the side chains compared to the bracelet forms, the probability distributions are very broad. Especially the annealed conformer is quite flexible, and many conformers of the isopropyl groups have similar energy. Nevertheless, the most favorable isopropyl torsional angles in the P1 conformer are similar to those found in the crystal.[26]

2.4. Calculated ROA and Raman Spectra

The calculations on the bracelet forms were based on the six valinomycin fragments containing four amino acids (L-Lac-L-Val-D-Hiv-D-Val and D-Hiv-D-Val-L-Lac-L-Val), so that the terminal molecular parts could be overlapped, and the end effects minimized in the CCT method.[19]

For the propeller and annealed conformers, many conformers are generated by isopropyl rotation (Tables S3 and S4, Supporting Information). Because all of them could not be calculated in a realistic time, a different fragmentation was used in this case. Three fragments containing five amino acid residues (L-Lac-L-Val-D-Hiv-D-Val-L-Lac) were used as the source of the force field and the Raman tensors (α), whereby only the L-Lac residues were fully overlapped with the neighboring fragments. Although some longer-distance interactions may be absent in this model, control computations indicated that the main spectral features were not affected. This can be seen in Figures S5 and S6 of the Supporting Information, in which ROA and Raman spectra of the P1 and A1 conformers calculated from the three fragments are compared to those calculated from the full set of six fragments. For the A1 conformer, the approximate calculation agrees well with the six-fragment one, except for the lowest part of the extended amide III region around 1270 cm^{-1}. Similarly, the approximation appears reasonable also for the P1 conformer, except for deviations of an ROA peak around 400 cm^{-1} and amide I Raman peaks in the P1 spectra. As discussed above, these spectral parts are not critical for elucidation of the structure. The three-fragment model works especially well for the annealed conformer, in which the amino acid residues are far apart and their vibrational modes do not couple.

The resultant ROA and Raman spectra of the propeller and annealed conformers are shown in Figures S7 and S8 of the Supporting Information. In this case spectra obtained by Boltzmann averaging of many conformers (WA in the figures) do not differ much from that of the most stable conformer (P1 or A1).

2.5. Free Valinomycin in Dioxane

Calculated ROA and Raman spectra of sB1, sB2, asB1, and asB2 are shown in Figure 4. Among the calculated ROA and Raman spectra for the backbone conformers in Figure 3, only the bracelet form has the characteristic ROA and Raman peaks observed experimentally. They all contain the characteristic ROA and Raman peaks, such as the $-/+/-$ ROA couplet of the methyl deformation, the broad $+/-/+$ ROA feature in the extended amide III region, the negative ROA peak of the isopropyl group at about 1000 cm^{-1}, the positive amide V ROA peak at about 345 cm^{-1}, and also the Raman peak at about 485 cm^{-1}.

In the whole wavenumber region the asB conformers provide better spectral shapes than the sB conformers. While sB1 species generate one sharp positive peak at 1344 cm^{-1} in the extended amide III region, the spectrum asB2 exhibits broad positive ROA peaks at 1354 and 1368 cm^{-1}, well related to the experiment. The isopropyl ROA bands observed between 1000 and 1200 cm^{-1} are also well reproduced by the asB but not by the sB conformers, and similarly for the asymmetric amide I Raman band. These results suggest that asB conformers are the dominant forms of free valinomycin in dioxane. Minor spectral features, however, also hint that the contribution of sB cannot be totally ignored. For example, in the region between 1265 and 1335 cm^{-1} the ROA spectrum of sB1 better agrees with the experimental one than that of asB.

To obtain more quantitative information about the conformer populations, the experimental ROA spectrum was decomposed[11] into wavenumber-scaled calculated ROA spectra (Figure 5). The fitted ROA spectrum agrees very well with the experimental one, except, for example, for the highest-frequency ROA band of the extended amide III region and some small peaks between 600 and 800 cm^{-1}. Large intensity deviations in Raman bands at 836, 1012, 1216, and 1303 cm^{-1} could be ascribed to solvent peaks not fully subtracted from the experimental spectrum. In agreement with the comparison with naked eye, the decomposition provided the asB conformers as dominant (ca. 70% for sum of asB1 and asB2), whereas sB conformers were the minor ones (ca. 30% for the sum of sB1 and sB2).

In the NMR studies[2,21,22] a symmetrical backbone structure of valinomycin was proposed to be dominant in nonpolar solvents. Because the asymmetric form cannot be distinguished by NMR due to the fast conformational exchange, our ROA analysis thus completes the knowledge about the behavior of this molecule. Indeed, as follows from observations based on ultrasonic absorption spectroscopy[27] at least two fast transitions should exist between three conformations with relaxation times of 2×10^{-9} and 2×10^{-8} s. The rate constants of the slowest transitions are about 10^7 s^{-1}. Migration of the weakened hydrogen bonds in the peptide backbone was proposed to be correlated to these fast transitions. Such interconversions among the conformers are clearly too fast to be detectable by

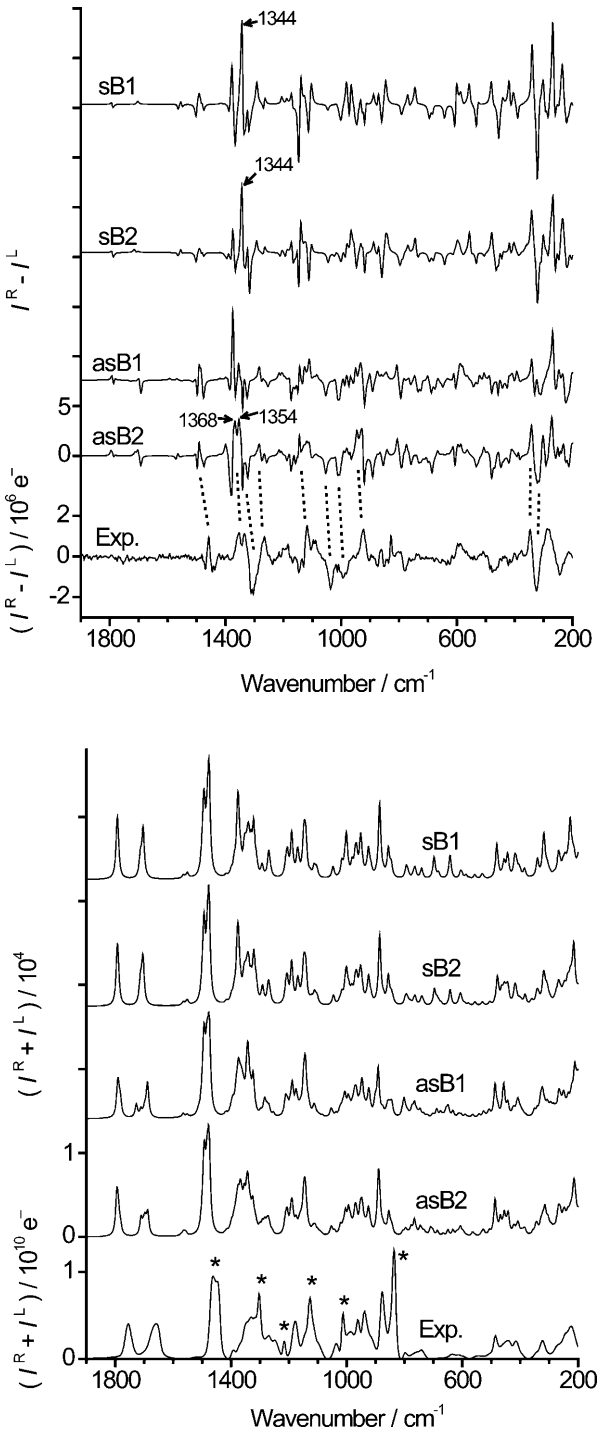

Figure 4. Calculated ROA (top) and Raman (bottom) spectra of the bracelet conformers of free valinomycin (sB1, sB2, asB1, and asB2; see Supporting Information for structural details) and the experimental spectra in dioxane. The asterisks in the Raman spectrum indicate peaks that strongly overlap with those of the solvents. The experimental intensity is presented as number of electrons detected by CCD; the calculated intensity is arbitrary.

NMR, unlike for ROA, for which the timescale (of the Raman scattering process, ca. 10^{-14} s) is much shorter.

The ultrasonic relaxation times[27] and the assignment to the migrating hydrogen bonds are in accord with the multiconformational model. Equilibrium exists among many asB structures that differ only in the position of the turn in the molecule. In time, the bending part of conformer asB (with 5→1 hydrogen bond instead of 4→1) migrates along the backbone. Furthermore, the minor sB conformations can be thought of as the intermediate state between the asB forms (asB↔sB↔asB′). To the best of our knowledge, there is no other analytical method as convenient as ROA that can provide the conformer populations and thus confirm these models. Obviously, further improvements of the accuracy of the ROA experiment and calculations are desirable to make the analysis more reliable.

Theoretical ROA and Raman spectra comprising averaging always agree better with the experiment than one-conformer spectra (Figures 4 and 5). For example, the negative deviation at the highest end of the extended amide III region of asB2 is canceled partly by the positive ROA peak of asB1 in the average. Also, contribution of the single positive peaks of the sB conformers at 1344 cm^{-1} to that of the asB2 conformer make the resultant peaks broader. As the DFT calculated vibrational frequencies are quite close to experiment, the scaling should not interfere with the band assignment.[11] The scaling factor used here was identical to that used for the valinomycin complex in methanol,[19] except for the amide I bands and the region between 1000 and 1100 cm^{-1}, where only poor agreement was achieved for the complex.

2.6. Free Valinomycin in Methanol

In Figure 6, Boltzmann-averaged ROA and Raman spectra calculated for the propeller and annealed backbone conformers are compared to the experimental spectra of valinomycin in methanol. Among the calculated ROA and Raman spectra of the backbone conformers in Figure 3, only the propeller matches reasonably the observed ROA and Raman peaks, such as the +/− ROA couplet of the methyl deformation bands, the broad +/−/+ ROA structure in the extended amide III region, the single negative amide V ROA peak at about 320 cm^{-1}, and the negative ROA peak at 876 cm^{-1}. The annealed conformer provides some peaks of opposite sign in the extended amide III region and lacks the positive ROA peak of the methyl deformation bands, the ROA signals between 1100 and 1250 cm^{-1}, and also the amide V ROA peak at about 320 cm^{-1}. The broad amide I Raman band of the amide carbonyl group can be reproduced by the propeller, but not by the annealed form. Thus we suppose that the propeller is dominant in methanol. However, some disagreements of the calculated ROA spectrum below 1250 cm^{-1} suggest large structural deviations from the ideal propeller backbone structure.

The cavity of the propeller form is open to solvent and accessible to methanol molecules. To consider the effect of the explicit solvation and structural fluctuation on the ROA and Raman spectra, calculated spectra were averaged for more MD snapshots. Combining MD and quantum mechanical calculations was found to be beneficial for small molecules in solution which exhibit similar flexible structure to valinomycin.[19,41,43] The ROA and Raman tensors and the force field of the P1 conformer were transferred to 17 MD geometries of the propeller

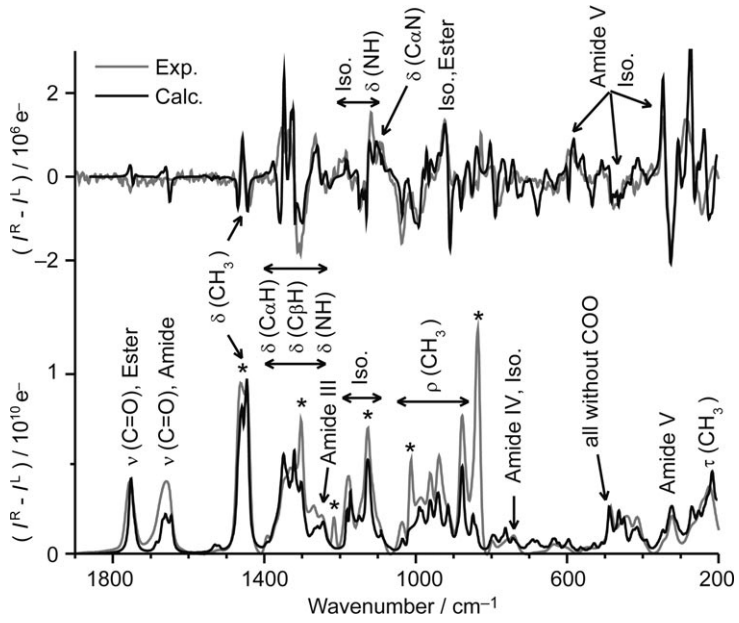

Figure 5. Fitted (black line) and experimental (gray line) ROA (top) and Raman (bottom) spectra of free valinomycin in dioxane. Conformer fractions obtained from the fitting are 34 (asB1), 39 (asB2), 14 (sB1), and 13% (sB2). Asterisks in the Raman spectrum indicate possible interference of solvent peaks. Main vibrational assignments are indicated; Iso. indicates the isopropyl group.

conformer and then averaged. In the MD run, the O···H distances of the 4→1 hydrogen bonds were kept constant, to maintain the propeller structure. Also the isopropyl torsion angles were restricted to those of the P1 conformer, to single out the effect of backbone fluctuation. Note that, in our experiments, although a relatively high concentration of 0.10 M was adopted, the corresponding number of solvent molecules of about 200 per valinomycin molecule still completely solvate the solute.

The MD-averaged ROA and Raman spectra (Figure 7, middle) better agree with the experimentally observed ones than the one-conformer spectrum (Figure 7, top). The ROA intensity and shape of the extended amide III region is nearly maintained after MD averaging, but intensities of the other ROA peaks decrease dramatically, especially for wavenumbers below 1000 cm^{-1}. The ROA bands between 1200 and 900 cm^{-1} become much simpler, in favor of experiment. The average Raman spectrum is broader throughout the entire region, except for the amide I bands. These simulations thus further support the conclusion that free valinomycin in methanol adopts

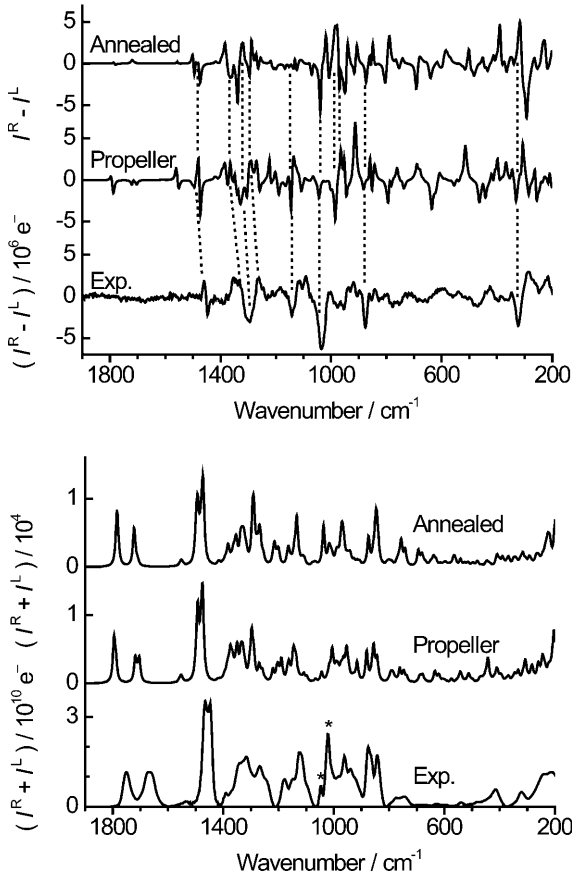

Figure 6. Calculated ROA (top) and Raman (bottom) spectra of the annealed and propeller conformers of free valinomycin, and the experimental spectra in methanol. Asterisks in the Raman spectrum indicate peaks that strongly overlap with those of the solvents.

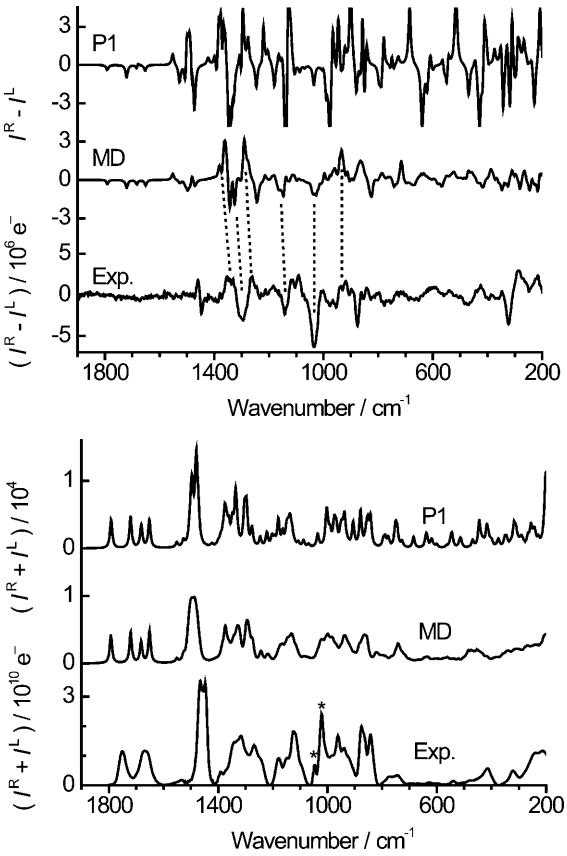

Figure 7. Calculated ROA (top) and Raman (bottom) spectra of conformer P1, averaged spectra from 17 MD snapshots, and experimental spectra of free valinomycin in methanol. Asterisks in the Raman spectrum indicate possible solvent interference.

flexible backbone structures, which can be derived from the canonical propeller conformer.

Characteristic MD snapshots for the propeller conformer are shown in Figure S9 of the Supporting Information. Whereas the three β-turns are maintained in these geometries, one or two regions of the propeller bend perpendicularly to a molecular plane. Some of them (marked by the blue line in Figure S9, Supporting Information) bend toward the inner cavity of valinomycin (forward in the projection), while others are bent backwards. The forward deviation was sometimes so large that the propeller structure approached the bracelet form. Because of the absence of polarization effects and other force-field terms the fluctuations can be overestimated by MD; nevertheless, the modeling is consistent with other data, and we assume that it at least qualitatively reproduces the flexibility of the molecule.

For practical computations, it is important to know the number of the MD geometries required for a converged result. Figures S10 and S11 (Supporting Information) show the convergence of the ROA spectrum as a function of the number of averaged MD snapshots *n*. Although reasonable spectral shape is achieved relatively fast (e.g., 10% error with 13 snapshots only), we can see that the overall dependence converges relatively slowly, approximately as $n^{-1/2}$. Many more geometries would be required for very accurate spectral intensities.[41,64]

2.7. Characteristic ROA Features of β-Turn of Valinomycin

The extended amide III band in ROA is sensitive to the secondary structures of proteins.[7,10,16,17,65] However, as shown for the valinomycin complex[19] and other systems,[12,43] this band can also be modulated by the side-chain signal. In particular, as it comprises the deformations of H_α, H_β, and NH, the ROA signal is strongly influenced by the side-chain torsion angle ($\angle H_\alpha C_\alpha C_\beta H_\beta$). Valinomycin is thus a convenient system for which the origin of this marker band can be analyzed in detail.

For example, the sB2 conformer has a sharp +/− ROA couplet at this region, the same as the complex (conformer II in ref. [19]). The backbone structures of these two conformers are slightly different (Table 1), but both of them have six repeating β-turns. The asB2 conformer, which has a deformed backbone and only five β-turns, exhibits broader and higher-frequency ROA bands. Finally, the propeller conformer with three β-turn structures has nearly the same broad +/− ROA couplet as asB2. The side-chain torsional angles of the propeller are not identical to those in asB (Tables S2 and S3, Supporting Information), but backbone geometries of the core residues of the β-turn, L-Val, and D-Hiv, are nearly the same as in the bracelet (Table 1). Only the annealed conformer without any β-turn exhibits a very different ROA band shape. Thus we can conclude that pure β-turn secondary structure is accompanied by a very sharp and close +/− ROA couplet in the extended amide III region, as observed in the valinomycin complex and sB conformers. This couplet becomes broader by fluctuation of the β-turn backbone, or by mixing with the signal of the backbone parts not involved in the turn.

3. Conclusions

The ROA experiments combined with quantum mechanical calculations gave interesting insight into the backbone structure and flexibility of free valinomycin in dioxane and methanol. The asymmetrical backbone structure of the bracelet form is more favored in dioxane than the canonical symmetrical one. The result thus somewhat contradicts the conclusions of previous NMR studies, which, however, can be reconciled by realizing that the asymmetrical form would be invisible for NMR. Unlike NMR, the ROA technique can also resolve conformers undergoing very fast exchange.

In methanol, structures based on the propeller conformer dominate. As follows from the combined MD/QM simulations, the structure is quite flexible and contains unstable β-turn regions. The opened propeller structure allows for strong solute–solvent interaction in methanol.

The sharp and close +/− ROA couplet at the extended amide III band observed in the symmetrical bracelet form of valinomycin was identified with a backbone structure similar to a β-turn. Broadening of this band, observed in the asymmetric bracelet and propeller forms, comes most probably from a distorted β-turn or from a signal of other backbone parts.

The results thus demonstrate the high sensitivity of ROA to the details of backbone structure. The combination of the experiments and theoretical modeling provided a valuable insight into the solution structure of the pseudo-peptide. Nevertheless, further improvement of the accuracy of the calculations and higher sensitivity of the experiment are desirable, especially for structural analyses of flexible biomolecules.

Acknowledgements

This study was performed with the support from the Academy of Sciences (M200550902, IAA400550702), Grant Agency of the Czech Republic (P208/11/0105), the Global COE Program Bio-Environmental Chemistry (to S.Y.), Luna, Metacentrum, and University of Tromsø computer facilities. Special thanks are addressed to Prof. Werner Hug from University of Fribourg, Switzerland, who kindly helped us to use his ROA spectrometer.

Keywords: conformational analysis · density functional calculations · molecular dynamics · Raman spectroscopy · valinomycin

[1] M. M. Shemyakin, N. A. Aldanova, E. I. Vinogradova, M. Y. Feigina, *Tetrahedron Lett.* **1963**, *4*, 1921 – 1925.
[2] M. M. Shemyakin, Y. A. Ovchinnikov, V. T. Ivanov, V. K. Antonov, E. I. Vinogradova, A. M. Shkrob, G. G. Malenkov, A. V. Evstratov, I. A. Laine, E. I. Melnik, I. D. Ryabova, *J. Membr. Biol.* **1969**, *1*, 402 – 430.
[3] S. Krasne, G. Eisenman, G. Szabo, *Science* **1971**, *174*, 412 – 415.
[4] L. D. Barron, A. D. Buckingham, *Mol. Phys.* **1971**, *20*, 1111 – 1119.
[5] L. D. Barron, M. P. Bogaard, A. D. Buckingham, *J. Am. Chem. Soc.* **1973**, *95*, 603 – 605.
[6] L. D. Barron, *Molecular Light Scattering and Optical Activity*, 2nd ed., Cambridge University Press, Cambridge, **2004**.
[7] L. D. Barron, A. D. Buckingham, *Chem. Phys. Lett.* **2010**, *492*, 199 – 213.
[8] J. Haesler, I. Schindelholz, E. Riguet, C. G. Bochet, W. Hug, *Nature* **2007**, *446*, 526 – 529.

[9] G. Zuber, W. Hug, *Helv. Chim. Acta* **2004**, *87*, 2208 – 2234.
[10] L. D. Barron, L. Hecht, E. W. Blanch, A. F. Bell, *Prog. Biophys. Mol. Biol.* **2000**, *73*, 1 – 49.
[11] M. Buděšínský, P. Daněček, L. Bednárová, J. Kapitán, V. Baumruk, P. Bouř, *J. Phys. Chem. A* **2008**, *112*, 8633 – 8640.
[12] J. Kapitán, V. Baumruk, V. Kopecký, Jr., P. Bouř, *J. Am. Chem. Soc.* **2006**, *128*, 2438 – 2443.
[13] W. Hug, G. Hangartner, *J. Raman Spectrosc.* **1999**, *30*, 841 – 852.
[14] W. Hug, *Appl. Spectrosc.* **2003**, *57*, 1 – 13.
[15] K. Ruud, A. J. Thorvaldsen, *Chirality* **2009**, *21*, E54-E67.
[16] I. H. McColl, E. W. Blanch, L. Hecht, L. D. Barron, *J. Am. Chem. Soc.* **2004**, *126*, 8181 – 8188.
[17] I. H. McColl, E. W. Blanch, A. C. Gill, A. G. O. Rhie, M. A. Ritchie, L. Hecht, K. Nielsen, L. D. Barron, *J. Am. Chem. Soc.* **2003**, *125*, 10019 – 10026.
[18] C. Toniolo, F. Formaggio, S. Tognon, Q. B. Broxterman, B. Kaptein, R. Huang, V. Setnička, T. A. Keiderling, I. H. McColl, L. Hecht, L. D. Barron, *Biopolymers* **2004**, *75*, 32 – 45.
[19] S. Yamamoto, M. Straka, H. Watarai, P. Bouř, *Phys. Chem. Chem. Phys.* **2010**, *12*, 11021 – 11032.
[20] M. Diem, *Introduction to Modern Vibrational Spectroscopy*, Wiley, New York, **1993**.
[21] V. F. Bystrov, Y. D. Gavrilov, V. T. Ivanov, Y. A. Ovchinnikov, *Eur. J. Biochem.* **1977**, *78*, 63 – 82.
[22] D. Patel, A. E. Tonelli, *Biochemistry* **1973**, *12*, 486 – 496.
[23] K. Neupert-Laves, M. Dobler, *Helv. Chim. Acta* **1975**, *58*, 432 – 442.
[24] E. G. Hutchinson, J. M. Thornton, *Protein Sci.* **1994**, *3*, 2207 – 2216.
[25] I. L. Karle, *J. Am. Chem. Soc.* **1975**, *97*, 4379 – 4386.
[26] I. L. Karle, J. L. Flippen-Anderson, *J. Am. Chem. Soc.* **1988**, *110*, 3253 – 3257.
[27] E. Grell, T. Funck, *J. Supramol. Struct.* **1973**, *1*, 307 – 335.
[28] T. Helgaker, K. Ruud, K. L. Bak, P. Jørgensen, J. Olsen, *Faraday Discuss.* **1994**, *99*, 165 – 180.
[29] K. Ruud, T. Helgaker, P. Bouř, *J. Phys. Chem. A* **2002**, *106*, 7448 – 7455.
[30] V. Liegeois, K. Ruud, B. Champagne, *J. Chem. Phys.* **2007**, *127*, 204105.
[31] L. D. Barron, A. R. Gargaro, L. Hecht, P. L. Polavarapu, *Spectrochim. Acta Part A* **1991**, *47*, 1001 – 1016.
[32] P. L. Polavarapu, *J. Phys. Chem.* **1990**, *94*, 8106 – 8112.
[33] G. Zuber, W. Hug, *J. Phys. Chem. A* **2004**, *108*, 2108 – 2118.
[34] W. Hug, G. Zuber, A. Meijere, A. F. Khlebnikov, H.-J. Hansen, *Helv. Chim. Acta* **2001**, *84*, 1 – 21.
[35] P. Bouř, V. Baumruk, J. Hanzlíková, *Collect. Czech. Chem. Commun.* **1997**, *62*, 1384 – 1395.
[36] S. Luber, M. Reiher, *J. Phys. Chem. B* **2010**, *114*, 1057 – 1063.
[37] P. Bouř, J. Sopková, L. Bednárová, P. Maloň, T. A. Keiderling, *J. Comput. Chem.* **1997**, *18*, 646 – 659.
[38] P. Bouř, T. A. Keiderling, *J. Phys. Chem. B* **2005**, *109*, 23687 – 23697.
[39] J. Kubelka, T. A. Keiderling, *J. Am. Chem. Soc.* **2001**, *123*, 12048 – 12058.
[40] V. Andrushchenko, H. Wieser, P. Bouř, *J. Phys. Chem. B* **2002**, *106*, 12623 – 12634.
[41] J. Kaminský, J. Kapitán, V. Baumruk, L. Bednárová, P. Bouř, *J. Phys. Chem. A* **2009**, *113*, 3594 – 3601.
[42] J. Kaminský, J. Šebek, P. Bouř, *J. Comput. Chem.* **2009**, *30*, 983 – 991.
[43] J. Hudecová, J. Kapitán, V. Baumruk, R. P. Hammer, T. A. Keiderling, P. Bouř, *J. Phys. Chem. A* **2010**, *114*, 7642 – 7651.
[44] A. D. Becke, *J. Chem. Phys.* **1993**, *98*, 5648 – 5652.
[45] J. P. Perdew, K. Burke, Y. Wang, *Phys. Rev. B* **1996**, *54*, 16533 – 16539.
[46] M. Govindarajan, K. Ganasan, S. Periandy, S. Mohan, *Spectrochim. Acta Part A* **2010**, *76*, 12 – 21.
[47] P. Daněček, P. Bouř, *J. Chem. Phys.* **2007**, *126*, 224513.
[48] X. Xu, W. A. I. Goddard, *J. Phys. Chem. A* **2004**, *108*, 2305 – 2313.
[49] J. W. Ponder in *Tinker, Software Tools for Molecular Design*, Washington University School of Medicine, **2000**.
[50] J. Wang, P. Cieplak, P. A. Kollman, *J. Comput. Chem.* **2000**, *21*, 1049 – 1074.
[51] A. Becke, *Phys. Rev. A* **1988**, *38*, 3098 – 3100.
[52] *Gaussian 09*, *Revision A.02*, M. J. Frisch, G. W. Trucks, H. B. Schlegel, G. E. Scuseria, M. A. Robb, J. R. Cheeseman, G. Scalmani, V. Barone, B. Mennucci, G. A. Petersson, H. Nakatsuji, M. Caricato, X. Li, H. P. Hratchian, A. F. Izmaylov, J. Bloino, G. Zheng, J. L. Sonnenberg, M. Hada, M. Ehara, K. Toyota, R. Fukuda, J. Hasegawa, M. Ishida, T. Nakajima, Y. Honda, O. Kitao, H. Nakai, T. Vreven, J. Montgomery, J. A., J. E. Peralta, F. Ogliaro, M. Bearpark, J. J. Heyd, E. Brothers, K. N. Kudin, V. N. Staroverov, R. Kobayashi, J. Normand, K. Raghavachari, A. Rendell, J. C. Burant, S. S. Iyengar, J. Tomasi, M. Cossi, N. Rega, N. J. Millam, M. Klene, J. E. Knox, J. B. Cross, V. Bakken, C. Adamo, J. Jaramillo, R. Gomperts, R. E. Stratmann, O. Yazyev, A. J. Austin, R. Cammi, C. Pomelli, J. W. Ochterski, R. L. Martin, K. Morokuma, V. G. Zakrzewski, G. A. Voth, P. Salvador, J. J. Dannenberg, S. Dapprich, A. D. Daniels, Ö. Farkas, J. B. Foresman, J. V. Ortiz, J. Cioslowski, D. J. Fox, Gaussian, Inc., Wallingford CT, **2009**.
[53] P. Bouř, T. A. Keiderling, *J. Chem. Phys.* **2002**, *117*, 4126 – 4132.
[54] P. Bouř, *Collect. Czech. Chem. Commun.* **2005**, *70*, 1315 – 1340.
[55] M. Buděšínský, J. Šebestík, L. Bednárová, V. Baumruk, M. Šafařík, P. Bouř, *J. Org. Chem.* **2008**, *73*, 1481 – 1489.
[56] J. Kapitán, V. Baumruk, V. Kopecký, Jr., P. Bouř, *J. Phys. Chem. A* **2006**, *110*, 4689 – 4696.
[57] J. Kapitán, V. Baumruk, V. Kopecký, Jr., R. Pohl, P. Bouř, *J. Am. Chem. Soc.* **2006**, *128*, 13451 – 13462.
[58] I. H. McColl, E. W. Blanch, L. Hecht, N. R. Kallenbach, L. D. Barron, *J. Am. Chem. Soc.* **2004**, *126*, 5076 – 5077.
[59] J. Kapitán, V. Baumruk, H. Hulačová, P. Maloň, *Vib. Spectrosc.* **2006**, *42*, 88 – 92.
[60] P. Mukhopadhyay, G. Zuber, D. N. Beratan, *Biophys. J.* **2008**, *95*, 5574 – 5586.
[61] P. Bouř, *J. Chem. Phys.* **2004**, *121*, 7545 – 7548.
[62] K. J. Jalkanen, I. M. Degtyarenko, R. M. Nieminen, M. Cao, L. A. Nafie, F. Zhu, L. D. Barron, *Theor. Chem. Acc.* **2008**, *119*, 191 – 210.
[63] K. J. Jalkanen, R. M. Nieminen, K. Frimand, J. Bohr, H. Bohr, R. C. Wade, E. Tajkhorshid, S. Suhai, *Chem. Phys.* **2001**, *265*, 125 – 151.
[64] P. Bouř, T. A. Keiderling, *J. Chem. Phys.* **2003**, *119*, 11253 – 11262.
[65] C. R. Jacob, S. Luber, M. Reiher, *Chem. Eur. J.* **2009**, *15*, 13491 – 13508 and ref [2].

Received: November 1, 2010
Revised: January 18, 2011
Published online on March 7, 2011

